# Paper II

Arch. Hydrobiol. 157 4 455–471 Stuttgart, July 2003

# Extracting signals of predation and competition from paired plankton time series

Gunnar Sandvik, Knut L. Seip[1] and Harald Pleym

With 8 figures and 3 tables

**Abstract:** Although competition and predation among plankton in seasonal aquatic systems must be ubiquitous, it remains a challenge to actually identify these interactions and to evaluate their relative strengths. Based on paired time series for zooplankton and phytoplankton in three lakes: Mjøsa (12 years), Farris (2 years) and Lake Washington (29 years), we construct phase portraits and quantitatively analyse their trajectories in an attempt to characterize interaction types and strengths. Because we can infer the type of interactions each pair partake in à priori (e.g., a phytoplankton/zooplankton pair is a prey/predator pair), we hypothesize that it is possible to distinguish trajectories resulting from a pair that compete from those of a pair constituting a prey/predator pair. We found that competition and predation can be distinguished based on the time series of the interacting species' biomass. Break points in population trajectories (i.e., population collapse) and the counter clockwise rotation of the trajectory in the phase portrait give the strongest signals of predation and the signals correspond to what we expect from classical predation theory. For competition we can only give plausible biological interpretations of identified signals, since signals from grazing, seasonality and competition are confounded.

**Key words:** time series, predation, competition, plankton, seasonal, simulation.

## Introduction

Quantitative identification and determination of the strength of species interactions, like predation and competition, have proven difficult in most natural systems (SARNELLE 1994, THOMPSON 1999). An important reason for this is that deterministic and stochastic physical forces interfere with the biological interactions (SEIP & REYNOLDS 1995). Chemostat studies have shown that even simple 2–3 species systems of algae and bacteria can display different interaction patterns with only incremental changes in nutrient supply and/or light intensity (MEGEE 1972, GURUNG et al. 1999).

[1] **Authors' address:** Høgskolen i Oslo, Cort Adlersgt 30, 0254 Oslo, Norway.
E-mail: knut.lehre.seip@iu.hio.no

DOI: 10.1127/0003-9136/2003/0157-0455 0003-9136/03/0157-0455 $ 4.25

Despite the high complexity of biological interactions in lakes that are driven by seasonal forces, several authors have found patterns in biomass time series that are suggestive of particular types of interactions (McCauley & Murdoch 1987, Matveev 1995, Jost & Arditi 2000, 2001). This study aims to develop and test a method that can distinguish "signals" that indicate the type and strength of interactions based on time series for pairs of organisms.

Seip (1997) developed and tested a method for characterizing ecological interactions from observed data. The method presented here, the angle frequency method (AFM), is an extension of the former. In a modelling study, Sandvik et al. (2002) found that four standard two species interactions (competition, predation, mutualism and facilitation) could all be distinguished by their biomass trajectories. Furthermore, signals in the trajectories that were characteristic for each interaction type could be identified. However, this was a deterministic study and results are not automatically relevant here.

In the present work, we study biomass time series data obtained from three lakes undergoing seasonal changes: mesotrophic Lake Mjøsa, Norway, (1986–1998), the mesotrophic to oligotrophic Lake Farris, Norway, (1982–1983), and Lake Washington, USA, (1962–1992), the latter had recovered from heavy eutrophication by 1975 (Edmondson & Lehman 1981).

Under the condition that each pair of plankton biomass time series à priori represents predation or competition, our hypothesis is that one can, based on these time series only, distinguish between signals generated by competition among phytoplankton species (PP) and predation by zooplankton on phytoplankton (ZP; i.e., that there are "events" in the time series being characteristic for each interaction type). In this study, we know à priori which time series represent predation and which represent competition. We examine if the ability to distinguish between two interaction types would be highest in data based on frequent samples at the species level or in aggregated data. We analyse individual species biomass (B = 0) for phytoplankton and zooplankton data, aggregated at a functional group level (e.g., Cyanophycea, Baciallariophyceae, Cladocera), (B = 1), as biomass of phytoplankton subdivided into large (>50 μm) and small (<50 μm) species (B = 2), and lastly, as total biomass of phytoplankton (large and small) and zooplankton, (B = 3). The time series are based on monthly samples, (T = 0) and on annual averages, (T = 1).

## Materials and methods

### The systems analysed, 3 seasonal lakes and 1 simulated seasonal system

Data from Lake Mjøsa are obtained from the station Skreia, in a large-scale national monitoring program (Kjellberg 1986–1998). Plankton counts (mixed samples from

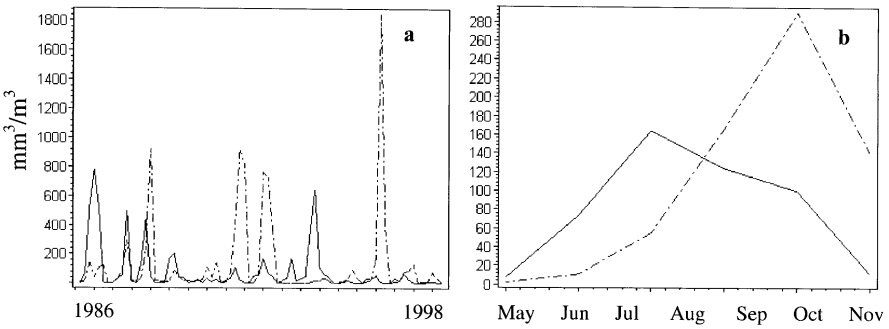


**Fig. 1.** Phytoplankton biomass as function of time, **a)** for the dominating phytoplankton species in lake Mjøsa (full line is *Asterionella formosa*, dashed line is *Tabellaria fenestrata,* **b)** the same data presented as monthly averages over the period 1986 to 1998.

the upper 10 m) are all reduced to arithmetic averages over one month, giving us 6 annual counts (May–October). Biomass time series are plotted for two of the most abundant species in Lake Mjøsa, demonstrating high variation in magnitude and timing of maximal annual biomass (Fig. 1). Using this data set, we test the effect of biological and temporal data aggregation (B = 0 to B = 3 and T = 0 and T = 1).

Data from Lake Farris are taken from routine water quality surveillances in 1982 and 1983 (HOLTAN et al. 1985). Mixed samples from the upper 10 m are taken monthly from May to September. These data are analysed at species level (B = 0) and with monthly sampling (T = 0) to see if predation and competition can be detected in a data set that is representative for most lake studies, (sampling for only 2 consecutive years).

The time series from Lake Washington is very long (1962–1991; EDMONDSON 1996), but of relatively coarse biological resolution (i.e., crustaceans, blue greens, rotatoria). These data are analysed at the functional group level (B = 1) and with monthly sampling (T = 0). Since the biological composition of Lake Washington changed with time as a result of nutrient abatement efforts for this lake, the main analysis is for the data divided into four time periods (1962–1969, 1970–1976, 1978–1983 and 1984–1990) and for the year 1979, which represents a year well after the nutrient abatement measures had been initiated.

We include two simulated prototype phase portraits of competition (C-S) and predation (P-S) in all our analyses. We obtain these "standards" by averaging biomass data from two sets of simulated time series (one for predation and one for competition), each set with eight parameter selections, varying carrying capacities, competition coefficients and niche differences (details in SANDVIK et al. 2002).

## Selection of species

From Lake Mjøsa and Lake Farris we select dominant species that occur each year and each month of the growing season. For the numerous species that occur sporadically and only for short periods, we cannot establish paired data sets. Table 1 shows the

**Table 1.** Months when species in Lake Mjøsa and Lake Farris reach their maximum biomass, their number in the seasonal phytoplankton and zooplankton successions and their maximal biomass during the respective period of observation.

| Lake Mjøsa | | | | Lake Farris | | | |
|---|---|---|---|---|---|---|---|
| Species | Month of maximum biomass | No. in seasonal succession (P#, Z#)* | Max. Biomass P in ($mm^3/m^3$) Z in (mg $dw/m^2$) (0–50 m) | Species | Month of maximum biomass | No. in seasonal succession (P#, Z#) | Max. Biomass P in ($mm^3/m^3$) Z in (mg $dw/m^2$) (0–50 m) |
| *Asterionella formosa* | July | P 2 | P(164) | small *chrysomonades* | June | P 2 | P(106) |
| *Tabellaria fenestrata* | September | P 3 | P(291) | large *chrysomonades* | May | P 1 | P(21) |
| *Rhizolenia longiseta* | July | P 2 | P(7) | *Gymnodinium* cf. *lacustre* | May | P 1 | P(8) |
| *Rhodomonas lacustris* | June | P 1 | P(59) | *Rhodomonas lacustris* | May<br>September | P 1<br>P 3 | P(16) May<br>P(18) September |
| *Eudiaptomus gracilis* | August | Z 2 | Z(1148) | *Holopedium gobberium* | July | Z 2 | Z(14) |
| *Mesocyclops leuckarti* | August | Z 2 | Z(723) | *Cyclops scutifer* | May<br>September | Z 1<br>Z 3 | Z(46) May<br>Z(47) September |
| *Bosmina longispina* | July | Z 1 | Z(1200) | *Eudiaptomus gracilis* | May | Z 1 | Z(34) |
| *Dapnia longispina* | September | Z 3 | Z(281) | *Bosmina longispina* | July | Z 2 | Z(30) |

* P = Phytoplankton nr; Z = Zooplankton nr.

months when the species reach their maximum during the season, their number in the seasonal succession (among species analysed here), and the maximal seasonal average biomass they obtain. Table 2 shows a list of the phase portraits analysed and the pairs of species (or units of higher biological aggregation).

Not all pairs of species in a lake are likely candidates for showing competition or prey predation patterns. We want to restrict our study to only relevant pairs (i.e., phytoplankton species that bloom in May to July and zooplankton that reach seasonal maxima in July or later). For instance the algae *Tabellaria fenestrata*, found at high population densities in Lake Mjøsa, normally blooms very late in the season (Table 1).

The zooplankton species *Bosmina longispina* in Lake Mjøsa and *Eudiaptomus gracilis* in Lake Farris achieve, for zooplankton, high densities very early, and phase portraits combining these zooplankton species with a phytoplankton that blooms later in the summer will not reflect a prey/predation interaction. For lake Mjøsa, for example, removing pairs including *T. fenestrata* or *B. longispina* reduces the number of pairs from 22 to 12.

## The angle frequency method (AFM)

To analyze the time series data, we use the angle class frequency method (AFM) developed in an early version by Seip (1997) and further developed and described in full by Seip & Pleym (2000) and Sandvik et al. (2002). The rationale for the AFM is the assumption that various types of interactions will show unique signals in phase space.

**Table 2.** Phase portraits analyzed. PP is competition between phytoplankton and ZP is predation by zooplankton on phytoplankton. B = 0 is species, B = 1 is functional group, B = 2 is small phytoplankton vs. large phytoplankton and any of the two size classes of phytoplankton vs. zooplankton, B = 3 is phytoplankton vs. zooplankton, T = 0 is monthly samples, T = 1 is annual samples.

| Lake Mjøsa (B = 0, T = 0) | | Lake Farris (B = 0, T = 0) | | Lake Washington (B = 1, T = 1) | |
|---|---|---|---|---|---|
| Predation | Competition | Predation | Competition | Predation | Competition |
| ZP1 Ast vs. Dap L | PP1 Ast vs. Tab | ZP1 Chs vs. Eud | PP1 Chs vs. Chl | ZP1 Blue vs. Rot | PP1 Blue vs. Green |
| ZP2 Ast vs. Bos | PP2 Ast vs. Rhi | ZP2 Chs vs. Cyc | PP2 Chs vs. Rho | ZP2 Blue vs. Cru | PP2 Blue vs. Dia |
| ZP3 Ast vs. Mes | PP3 Ast vs. Rho | ZP3 Chs vs. Hol | PP3 Chs vs. Gym | ZP3 Blue vs. Dap | PP3 Green vs. Dia |
| ZP4 Ast vs. Eud | PP4 Tab vs. Rhi | ZP4 Chs vs. Bos | PP4 Chl vs. Rho | ZP4 Green vs. Rot | |
| ZP5 Tab vs. Dap L | PP5 Tab vs. Rho | ZP5 Chl vs. Eud | PP5 Chl vs. Gym | ZP5 Green vs. Cru | |
| ZP6 Tab vs. Bos | PP6 Rhi vs. Rho | ZP6 Chl vs. Cyc | PP6 Rho vs. Gym | ZP6 Green vs. Dap | |
| ZP7 Tab vs. Mes | | ZP7 Chl vs. Hol | | ZP7 Dia vs. Rot | |
| ZP8 Tab vs. Eud | | ZP8 Chl vs. Bos | | ZP8 Dia vs. Cru | |
| ZP9 Rhi vs. Dap L | | ZP9 Rho vs. Eud | | ZP9 Dia vs. Dap | |
| ZP10 Rhi vs. Bos | | ZP10 Rho vs. Cyc | | | |
| ZP11 Rhi vs. Mes | | ZP11 Rho vs. Hol | | | |
| ZP12 Rhi vs. Eud | | ZP12 Rho vs. Bos | | | |
| ZP13 Rho vs. Dap L | | ZP13 Gym vs. Eud | | | |
| ZP14 Rho vs. Bos | | ZP14 Gym vs. Cyc | | | |
| ZP15 Rho vs. Mes | | ZP15 Gym vs. Hol | | | |
| ZP16 Rho vs. Eud | | ZP16 Gym vs. Bos | | | |

| Lake Mjøsa (B = 1) | | Lake Mjøsa (B = 2 and B = 3) | |
|---|---|---|---|
| ZP1 Dia vs. Cop | PP1 Dia vs. Din | ZP1 Sm vs. Zoo (B = 2) | PP1 La vs. Sm (B = 2) |
| ZP2 Dia vs. Cla | PP2 Dia vs. Green | ZP2 La vs. Zoo (B = 2) | |
| ZP3 Din vs. Cop | PP3 Din vs. Green | ZP3 Phyto vs. Zoo (B = 3) | |
| ZP4 Din vs. Cla | | | |
| ZP5 Green vs. Cop | | | |
| ZP6 Green vs. Cla | | | |

**Ast** = *Asterionella formosa,* **Eud** = *Eudiaptomus gracilis,* **Mes** = *Mesocyclops leuckarti,* **Bos** = *Bosmina longispina,* **Tab** = *Tabellaria fenestrata,* **Rhi** = *Rhizolenia longiseta,* **Rho** = *Rhodomonas lacustris,* **Dap L** = *Dapnia longispina,* **Chs** = small *chrysomonades* (>7), **Chl** = large *chrysomonades* (<7) **Gym** = *Gymnodinium cf. lacustre,* **Cyc** = *Cyclops scutifer,* **Hol** = *Holopedium gibberium,* **Blue** = Cyano bacteria, **Green** = Green algae, **Dia** = Diatoms, **Rot** = Rotatoria, **Dap** = Daphnia, **Cru** = Crustaceans, **Din** = Dinophycaea, **Cop** = Copepoda, **Cla** = Cladocera, **La** = large phytoplankton (>50 µm), **Sm** = small phytoplankton (<50 µm), **Zoo** = total zooplakton, **Phyto** = total phytoplankton.

For example, predation as defined by the Lotka Volterra equations, shows a counter clockwise rotation when the prey is depicted on the x-axis and the predator on the y-axis (GILPIN 1973, SEIP 1997, SEIP & PLEYM 2000).

Firstly, the phase portraits are divided into quadrants, these being defined by the average reading along both axes in the phase portrait. Secondly, we identify the angle formed by the trajectory between observations at two consecutive sampling times and the x-axis. These angles are distributed into classes of 18°, yielding histograms with 21 bars per quadrant. We use the term signal when referring to these classes of angles (one class is one signal). The histograms generated (one per pair of time series) are compared to identify signals associated with the interactions.

We use principal components analysis (PCA) to analyze these data (Unscrambler, version 6.11 b, CAMO ASA, Maple V, Release 5, Waterloo Maple, Inc.). From PCA, scores and loadings are obtained.

PCA scores give the relative distribution of objects (here, data from each of the paired time series) along PC1 and PC2. From these scores we calculate the centre-centre distance, D, for any two groups of data to be compared:

$$D = |g_1 + g_2| \tag{1}$$

where $g_1$ is the average score of group 1 and $g_2$ the average score for group 2 along a PC-axis. The score range, $R_n$, is then calculated as:

$$R_n = g_{\max} - g_{\min} \tag{2}$$

where $g_{min}$ is the lowest score and $g_{max}$ is the highest score (irrespective of groupings among scores) along a PC-axis. The percentage discrimination, $D_{\%}$, is calculated as:

$$D_{\%} = \frac{D * 100}{R_n} \tag{3}$$

A $D_{\%}$ value of = 100 implies that scores are separated as two distinct groups at opposite ends of the PC axis. A $D_{\%}$ value of ~0 represents no clustering of scores. $D_{\%}$

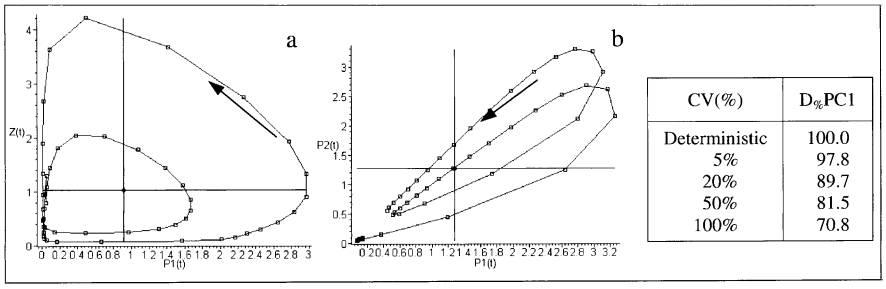


| CV(%) | D%PC1 |
|---|---|
| Deterministic | 100.0 |
| 5% | 97.8 |
| 20% | 89.7 |
| 50% | 81.5 |
| 100% | 70.8 |

**Fig. 2.** Simulated prey-predation **a)** and competition **b)** in seasonal environments and expressed as phase portraits demonstrating the vectorized trajectories by the AFM. The arrows show rotational direction of trajectories. Right table shows the sensitivity of the method to stochastic noise (observation error). With increasing stochastic noise applied to angle frequencies (expressed by coefficient of variation, CV). The discrimination measure, $D_{\%}$PC1, shows how well prey-predation is discriminated from competition.

values in the range 10–15 are found to be visually detectable by inspection of score plots.

PCA loadings relate the variables (here the 84 angle classes) to the PCA scores. Based on loadings associated with $g_1$ and $g_2$ scores evaluated for each separate analysis we define signal strength ($S_s$):

$$S_s = R_s * E_s \tag{4}$$

where $R_s$ is representability and $E_s$ is exclusivity of a signal over the lakes analyzed.

$$R_s = \frac{n_s}{N} \tag{5}$$

where $n_s$ is the number of lakes in which a certain signal is characteristic. N is the number of lakes analyzed (here 3). $R_s$ (range 0–1) give weight to signals that occur frequently.

$$E_s^{comp} = \frac{n_s^{comp}}{n_s^{pred} + 1}, \tag{6}$$

$$E_s^{pred} = \frac{n_s^{pred}}{n_s^{comp} + 1} \tag{7}$$

where $n_s^{comp}$ is the number of lakes in which a certain signal is characteristic for competition and $n_s^{pred}$ is the corresponding number for predation. $E_s$ (range 0–N) gives high weight to signals that are characteristic for only one interaction. High $S_s$ values (range 0–3) point to signals that are good candidates for identifying a given interaction type.

## Results

To reduce the number of figures we show selected score plots, which represent the three lakes and that show the best discrimination between predation and competition. However, the degree of discrimination, $D_{\%}$ is reported for all analyses.

Fig. 3 shows three typical phase space trajectories, two for competition and one for prey/predation. Lower graphs show full time series and upper graphs show aggregated time series. The full time series trajectories suggest that it is not evident that scores based on competition can be distinguished from scores based on prey/predation interactions.

### Analyses of PCA scores, irrelevant pairs of species removed

We first run an analysis at the species level and with monthly samples (B = 0, T = 0) for Lake Mjøsa and for Lake Farris, and at the aggregation level (B = 1,

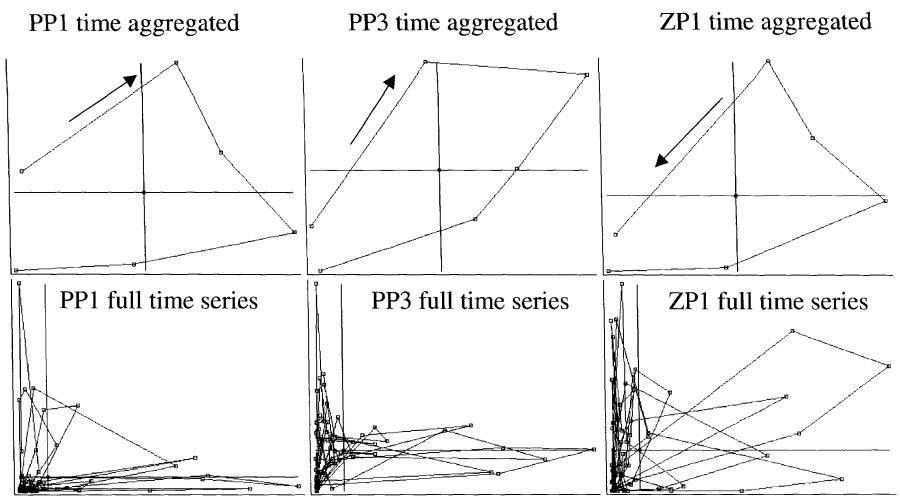


**Fig. 3.** Phase portraits of lake Mjøsa data, for competition PP1 (*Asterionella* vs. *Tabellaria*) and PP3 (*Asterionella* vs. *Rhodomonas*) and predation ZP1 (*Asterionella* vs. *Daphnia*). The first species of the pair (i.e., *Asterionella*) is depicted on the x-axis. Arrows show direction of rotation. Upper part of the panel trajectories shows average and normalized (1/SD) seasonal dynamics for the years 1986–1998 (each point in the upper phase portraits represents successive months from May to October). The lower panel shows the corresponding complete time series.

T = 1) for Lake Washington, since species level data are not available for the latter lake.

Lake Mjøsa phase portraits analysed with only relevant species pairs and without the prototypes P-S and C-S yield competition, PP, scores largely to the left and predation, ZP, scores largely to the right of the PCA score plot ($D_{\%}$PC1 = 52 and $D_{\%}$PC2 = 14, Fig. 4). The figure also shows the relationship between scores and loadings to be discussed below.

The Lake Farris data are analysed similarly and we obtain $D_{\%}$PC1 = 49 and $D_{\%}$ PC2 = 16 (Fig. 5).

Lake Washington data analysed as separate time periods (1–4) give low $D_{\%}$ values along PC1, (8, 11, 13, 6) and PC2, (20, 18, 2, 0), respectively. Score plots are not shown for this and the following analyses. Also for the randomly selected year 1979 we find the same trend, ($D_{\%}$PC1 = 2 and $D_{\%}$PC2 = 22). When we analyse the entire data set (1962–1991) we also receive low $D_{\%}$ values ($D_{\%}$PC1 = 1.4 and $D_{\%}$PC2=1.2).

### Analyses of PCA scores for all pairs in Lake Mjøsa

We analysed data from Lake Mjøsa in combinations of various aggregated forms (B = 0 to B = 3 and T = 0 to T = 1) by visually inspecting PCA score

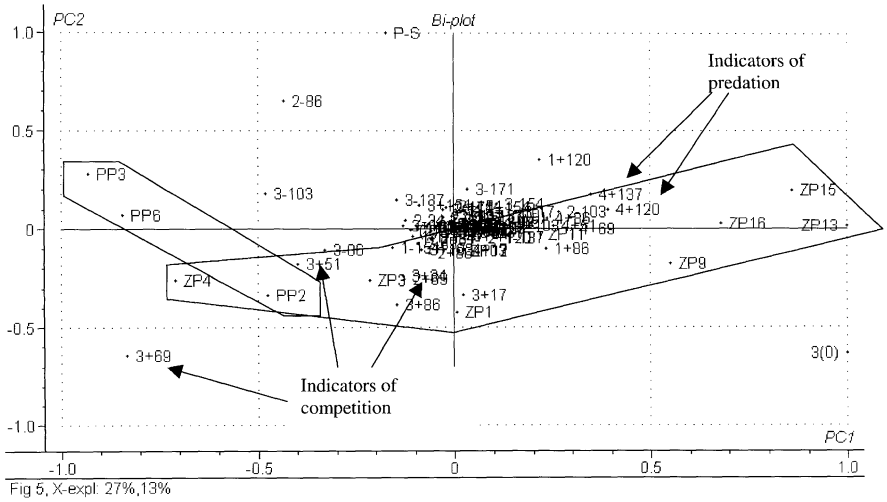


**Fig. 4.** Lake Mjøsa (B = 0, T = 0). The Principal Component Analysis, PCA bi-plot for full time series data without *Tabellaria fenestrata* and *Bosmina longispina*, shows predation by zooplankton species on phytoplankton species (ZP) and competition between pairs of phytoplankton (PP). Number following the pairs of letters refers to pair identification in Table 2. Model simulation of predation is included as P-S. Modeled competition C-S gave very different response and was not included in the plot to avoid compressing all other points into a corner. Angle brackets are identified by the numbers 1 to 4 for the quadrants, and by the numbers ± 180 for the mean angle within the quadrant (see text). The first principal component, PC1, explains 27 % of the variance, and the second component, PC2, explains 13 %.

plots and calculating $D_{\%}$ values. All $D_{\%}$ values are calculated from separate analyses without the simulated prototypes C-S and P-S included. Thus, the $D_{\%}$ values cannot always be read directly from graphs where the prototypes are included for reference. We do not show the graphs, but summarize the results for separation, $D_{\%}$, in Fig. 6. At the highest level of data aggregation (T = 1, B = 2 and B = 3) the scores for competition (PP) were positioned to the left and the three scores for prey/predation (ZP1 to ZP3) to the right. The scores for the two prototypes were not positioned consistently with the scores based on observations. The ZP scores are not independent at this level of aggregation, but the result remains that PP and ZP are at different ends of the PC1 axis ($D_{\%}$ = 97). At the same level of biological aggregation (B = 2), but with no temporal data aggregation (T = 0), the scores give a lower discrimination between PP and ZP. $D_{\%}$ is 45 along PC1 and 76 along PC2.

At the medium level of biological aggregation (functional group level), but without the temporal variability (B = 1, T = 1), the score plot separates the competition scores (PP1 to PP3) from the three prey/predation scores, ($D_{\%}$PC1 = 25 and $D_{\%}$PC2 = 46), here, it is PC2 that best picks up the signals

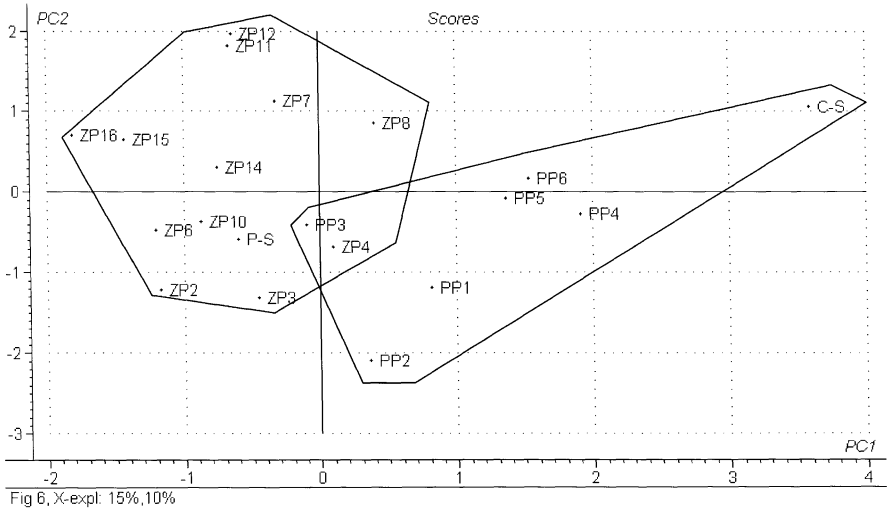


**Fig. 5.** Lake Farris (B = 0, T = 0). Principal component plot, PCA score plot for full time series data (T = 0) for the two consecutive years 1982 and 1983. The figure shows predation by zooplankton species on phytoplankton species (ZP) and competition between pairs of phytoplankton species (PP). Number following the pairs of letters refers to pair identification in Table 2. Model simulations of predation and competition are included as P-S and C-S, respectively. Loading plot not shown. The first principal component, PC1, explains 15 % of the variance, and the second component, PC2, explains 10 %.

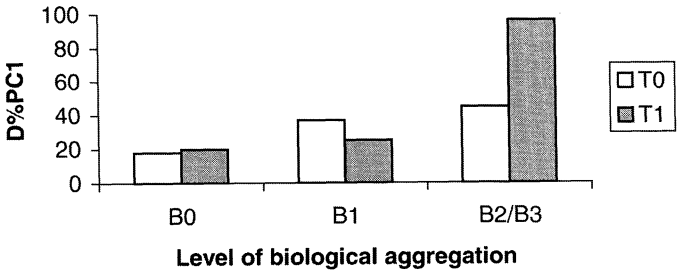


**Fig. 6.** $D_{\%}PC1$ results for lake Mjøsa analyses using various biological and temporal aggregations. B0 is no biological aggregation, B1 is aggregation at the functional group level, B2 is phytoplankton divided into small and large sizes, B3 is total biomass of phytoplankton and zooplankton. T0 is full time series and T1 is the generalized year.

from the interactions. The positions of P-S and C-S in the score plot indicate that at this aggregation level the model represents lake data fairly well. When temporal variability is included (B = 1, T = 0), the discrimination increases along PC1, but decreases along PC2 ($D_{\%}PC1 = 37$ and $D_{\%}PC2 = 21$).

At the species level (i.e., no biological aggregation), but with temporal aggregation (B = 0, T = 1), we find low discrimination and a slight tendency toward negative PP scores and positive ZP scores in the PC1 dimension ($D_{\%}PC1 = 20$ and $D_{\%}PC2 = 3$). Finally, when there is no aggregation in the data (B = 0, T = 0), the PCA analysis shows even lower discrimination between predation and competition ($D_{\%}PC1 = 18$ and $D_{\%}PC2 = 6$). ZP scores have more negative values than PP scores along PC1. We also find that P-S is closer to the centre of ZP scores than to the centre of PP scores. C-S, however, represents competition poorly.

Figure 6 shows a summary of the effects of temporal and biological aggregation on $D_{\%}PC1$ values in the Lake Mjøsa data. All these results suggest that data aggregation can amplify relevant signals and sort out noise.

### Analyses of PCA loadings

With only relevant pairs included, a number of angle classes are identified as indicative of competition and predation in the three systems analysed. Due to the low discrimination and high biological aggregation in the in Lake Washington data, we cannot à priori remove irrelevant species. We therefore removed PCA scores systematically from the set where all four-time periods were included until predation and competition clusters appeared in the plot, ending up with 16 pairs out of 55 pairs. Although this procedure is partly circular, when PCA loadings associated with these clusters are compared, signals became largely the same as for lake Mjøsa and Lake Farris (see Table 3).

When we use signal strength $S_s = 0.7$ as a minimum criterion for selecting strong indicative angles, three predation signals and five competition signals result. (This $S_s$ value is about 23 % of maximal possible $S_s$ value with 3 systems, $S_{smax} = 1 * 3$). Predation is associated with three angle classes of equal RE values ($S_s = 0.7$, Table 3); Signal P1, [−145 to −128] in the upper right quadrant (i.e., when both prey and predator are abundant the prey decline slightly faster than the predator), signal P2, [−111 to −94] in the upper left

**Table 3.** Summary of signals (angle brackets) of predation and competition identified for all lakes and sorted after decreasing $S_s$ values. $R_s$ = representability, $E_s$ = exclusivity, M = Lake Mjøsa, F = Lake Farris, W = Lake Washington.

| Predation | | | | | | | Competition | | | | | | |
|---|---|---|---|---|---|---|---|---|---|---|---|---|---|
| | Signal | | | | | | | Signal | | | | | |
| Angle bracket | ID | # | $R_s$ | $E_s$ | $S_s$ | Lakes | Angle bracket | ID | # | $R_s$ | $E_s$ | $S_s$ | Lakes |
| Q-I [−145 to −128] | P1 | 2 | 0.7 | 1 | 0.7 | M,W | Q-III [−180 to −162] | C1 | 3 | 1.0 | 3 | 3.0 | F,M,W |
| Q-II [−111 to −94] | P2 | 2 | 0.7 | 1 | 0.7 | F,M | Q-III [43 to 60] | C2 | 2 | 0.7 | 2 | 1.3 | F,M |
| Q-III [−25 to −8] | P3 | 2 | 0.7 | 1 | 0.7 | F,M | Q-III [60 to 77] | C3 | 2 | 0.7 | 2 | 1.3 | F,M |
| | | | | | | | Q-III [77 to 94] | C4 | 2 | 0.7 | 1 | 0.7 | F,M |
| | | | | | | | Q-IV [−180 to −162] | C5 | 2 | 0.7 | 1 | 0.7 | M,W |

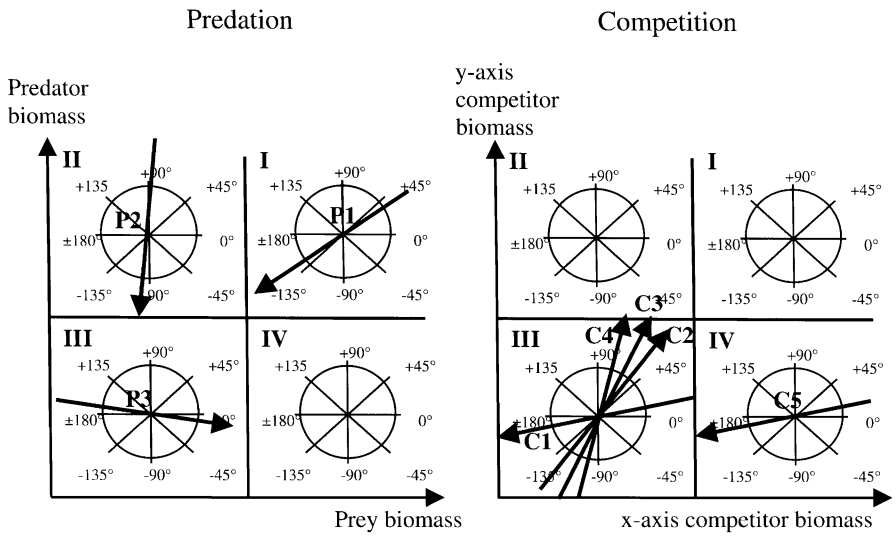


**Fig. 7.** Phase portraits for predation and competition divided into quadrants. The arrows show the approximate angle of the most characteristic angle brackets for each interaction (see text). Roman letters I, II, III and IV designate quadrant numbers. Arrows show angle that are characteristic for each interaction type in each quadrant (see Fig. 8 for a biological interpretation in terms of paired time series).

quadrant, (i.e., when predator is abundant and prey is rare the predator decline fast while the prey decline slowly), signal P3, [−25 to −8] in the lower left quadrant, (i.e., when both predator and prey are rare the prey grows fast, while the predator decrease slowly). Fig. 7 summarizes the results from the PCA loadings.

Five angle classes identify competition (Table 3). Four of these are found in the lower left quadrant (i.e., when both competitors are rare). The strongest competition signal C1 ($S_s = 3.0$) in angle class [−180 to −162] describes a situation where the competitors decline at different rates (early starter declines ~9 times faster than the late starter). The signals C2-C4 are adjacent angle classes. The signal C2 ($S_s = 1.3$), with angle class [43 to 60] describes a situation where both competitors increase (at approximately equal rates). The signal C3 ($S_s = 1.3$), with the angle class [60 to 77], describes a situation where the late starters increase about three times faster than the early starters. The signal C4 ($S_s = 0.7$), with the angle class [77 to 94], describes the situation where the late starter increases about ten times faster than the early starter. The fifth signal characteristic for competition C5 ($S_s = 0.7$) is angle class [−180 to −162] in the lower right quadrant (i.e., when the early starter is abundant and the late starter is rare, the early starter declines fast while the late starter declines slowly).

## Discussion and conclusions

Maintaining only those species that are reasonable candidates for showing competition or predation, discrimination improved about threefold for Lake Mjøsa and Lake Farris data compared to data sets with all species included. This finding supports the existence of characteristic signals for the two interaction types. Biological and temporal aggregations appear to improve the results if primary data at the species level are aggregated and when all pairs of species are included (i.e., the case B = 0 and T = 0). The results indicate that two growth seasons are sufficient to extract the relevant signals, even with monthly averages based on 1–3 samplings (Lake Mjøsa and Lake Farris). If data only can be obtained on the functional group level, as for Lake Washington, our results suggest that the strength of the signals is low and that the strength does not increase with length of time series in the range analysed here (1–30 years). We find that the species time series B = 0 is much less conclusive (in terms of $D_{\%}PC1$) than the biologically aggregated time series $B>0$. This may be due to the lower overall error in the mean when there are several measurements of the species (c.f., results of sensitivity analysis in Fig. 2).

### Interpretation of interaction signals

Each angle class discussed here represents the cumulative response ($S_s$ value) for plankton in all three-lake systems and prey and predator biomass are scaled to about the same biomass range. This implies that it is not possible to go back to individual time series to support the interpretation of the angle classes identified here.

Below, we interpret the angle classes found from examining the phase portraits by qualitatively relating them to central aspects of the PEG (Plankton Ecology Group) model of seasonal succession of planktonic events in fresh waters (SOMMERS et al. 1986) and the standard Lotka Volterra prey-predator model (Fig. 8 a and b). Although not explicitly stated, the PEG model incorporates "early starters" and "late starters". The former are r-strategists, growing fast in the spring, and are tolerant to environmental harshness, but they are weak competitors and susceptible to grazing. The "late starters" (K-strategist) grow slower in the spring and are sensitive to environmental harshness, but they grow faster and are strong competitors and less susceptible to grazing during midsummer (a strongly competitive environment in most seasonal lakes). The eight angle classes identified as strong signals ($S_s > 0.7$) in this study fit plausibly to the standard descriptions of competition and predation (Fig. 8), thus supporting the biological relevance of the identified signals.

The three angle classes identified as typical of predation are consistent with the classical counter-clockwise rotation of prey-predation trajectories

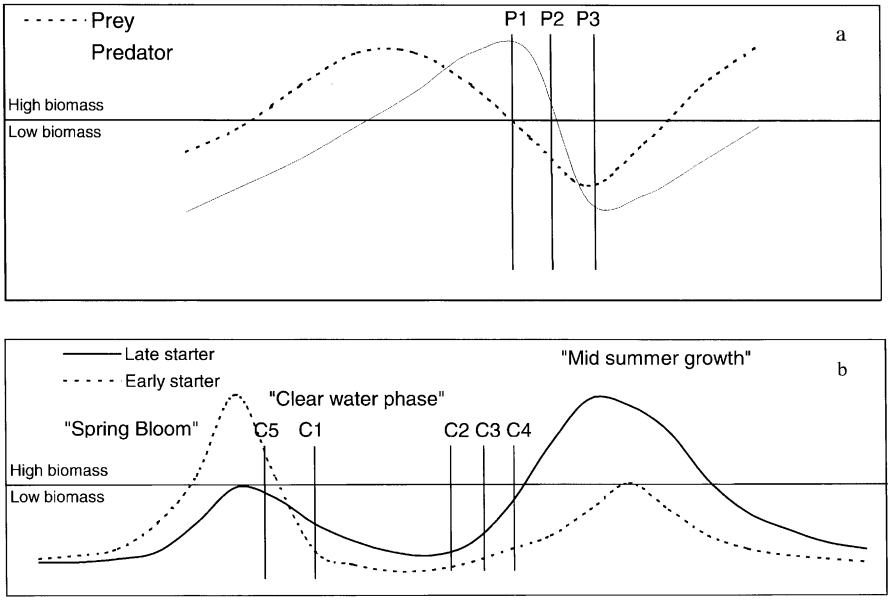


**Fig. 8.** Schematic time series showing prey-predator cycle **(a)** and competition between a pair of phytoplankton with niche difference ("early starter" and "late starter") in a seasonal lake **(b)**. Symbols P1-P3 and C1-C5 associate sections of the time series with angle brackets. P1 = [−145 to −128] in the upper right quadrant, P2 = [−94 to −111] in the upper left quadrant, P3 = [−25 to −8] in the lower left quadrant, C1 = [−162 to −180] in the lower left quadrant, C2 = [43 to 60] in the lower left quadrant and C3 = [60 to 77] in the lower left quadrant, C4 = [77 to 94] in the lower left quadrant and C5 = [−162 to −180] in the lower right quadrant. The horizontal line shows approximate demarcation line between "high" and "low" biomass.

(see Fig. 7). First, when both prey and predator are abundant, prey declines slightly faster than the predator. This signal (P1 in Table 3) may represent the predator being on the verge of collapsing because the prey (still in relatively high densities) is declining (Fig. 8 a, vertical line P1). Secondly, when predator is abundant and prey is rare and the predator declines approximately 3 times faster than the prey, the situation may correspond to a point in the predator-prey cycle where the predator is in the early collapse phase and the prey is still declining (Fig. 8 a, vertical line P2). Third, when both prey and predator have low densities, the prey grows relatively fast while the predator is still declining. This situation may represent the late predator collapse where the prey has regained positive net growth (Fig. 8 a, vertical line P3).

Considering angle classes indicative of competition, biological explanations appear less clear. However, given the analytical design and an understanding of the studied systems, we offer biologically plausible explanations for the five indicative angles we identified. Recall that we always designate

the species that reach its seasonal maximum first (early starter) as competitor 1 (x-axis).

First, when both competitors are rare, the early starter declines nine times faster than the late starter (signal C1, Table 3). There are two periods when both competitors normally have low and declining biomass: late spring bloom when both algae are grazed upon, and autumn when seasonal forces causes their decline. The huge difference in the rates of decline suggests that this angle class describes late spring bloom, because here the early starters have reached high populations, and (at vertical line C1, Fig. 8 b) virtually collapse because of heavy grazing leading to the "clear water phase". A relative shift in environmental state with time (to the benefit of the late starter) and potentially lower edibility in the late starter may also contribute to the large difference in the rates of decline. In late autumn, we would expect more similar rates of decline because reduction in light energy would impact the growth of all phytoplankton species negatively, as suggested by step 21 in the PEG model.

Second, when both competitors are rare, three adjacent angle classes indicate a range from almost equal growth rates in both competitors to the late starter growing much faster than the early starter. This may be the situation when the post "clear water" growth starts, (Fig. 8 b, vertical lines C2-C4). This interpretation is supported by the late starter growing faster than the early starter indicating a relative shift with time between environmental state and niche optimum favouring the late starter assumed to be a K-strategist. In accordance with the PEG model, step 5, the late starter may also be a less "edible" phytoplankton having a growth advantage after the "clear water" phase.

Third, when the abundant early starter decreases fast, the rare late starter decreases slowly (Fig. 8 b, vertical line C5). This signal is suggestive of an earlier section of the late spring bloom than expressed by signal C1. Again, heavy grazing and difference in susceptibility to grazing (late starter is assumed to be less susceptible) may give the biological rationale for this signal.

## General conclusion

We show that the AFM can successfully be used to study phase portraits representing biomass data from real ecosystems. For the lake Mjøsa data, we demonstrate that discrimination increases with both temporal and biological aggregation of data. For competition we found one signal, C1, that is common for all three lakes analysed (Table 3).

Predation can probably be distinguished for most pairs by inspection of clusters in PCA score plots and their accompanying loadings. Collapse in predator population at low prey densities seems to give the strongest signal of predation. Also the counter-clockwise rotation of identified signals suggests a

good correspondence between the Lotka–Volterra model and our results. For competition we can only give plausible biological interpretations of the signals that are identified as important. Competition signals are sensitive to the type of competitors represented by the axes in the phase portrait (i.e., r-strategist or K-strategist and susceptible or resistant to grazing). One of the five angle classes identified as important shows nearly equal growth from low populations of both competitors. This corresponds to the standard assumptions in a two species Lotka–Volterra competition model. Our results, however, also suggest that effects external to the interaction, like grazing and seasonality (see Fig. 8, b) are confounded with the effects of competition in our data. These latter effects can, however, be reasonably well accounted for when the assumed competition signals are interpreted in the context of the PEG model, since this model also incorporates these external effects.

Results are preliminary, but if additional analyses lend further support to our conclusions, this method has the potential to become a valuable tool for ecologists and environmental managers seeking to characterize important interactions in natural systems.

## Acknowledgements

We wish to thank CHRISTINE JESSUP at Stanford University and two anonymous reviewers for advice and discussion.

## References

EDMONDSON, W. T. (1996): Lake Washington Data. Lake Washington, Washington, USA. – University of Washington.

EDMONDSON, W. T. & LEHMAN, J. T. (1981): The effect of changes in the nutrient income on the condition of Lake Washington. – Limnol. Oceanogr. **26:** 1–29.

GILPIN, M. (1973): Do hares eat lynx? – Amer. Nat. **107:** 727–730.

GURUNG, T. B. URABE, J. & NAKANISHI, M. (1999): Regulation of the relationship between phytoplankton *Scenedesmus actus* and heterotrophic bacteria by the balance of light and nutrients. – Aquat. Microb. Ecol. **17:** 27–35.

HOLTAN, G., BRETTUM, P., LIEN, L. & LØVIK, J. E. (1985): Overvåkning i Farris-Siljanvassdraget 1982–1984. – Del A. Hovedrapport. Statlig program for forurensningsovervåking 186/85. (in Norwegian).

JOST, C. & ARDITI, R. (2000): Identifying Predator-Prey Processes from Time-Series. – Theor. Pop. Biol. **57:** 325–337.

– – (2001): From pattern to process: identifying predator-prey models from time series data. – Popul. Ecol. **43:** 229–243.

KJELLBERG, G. (1986–1998): Tiltaksorientert overvåkning av Mjøsa med tilløpselver. – Statlig program for forurensningsovervåkning, NIVA/SFT. (in Norwegian).

MATVEEV, V. (1995): The dynamics and relative strength of bottom-up vs. top-down impacts in a community of subtropical lake plankton. – Oikos **73:** 104–108.

McCauley, E. & Murdoch, W. W. (1987): Cyclic and stable populations: Plankton as a paradigm. – Amer. Nat. **129:** 97–121.

Megee, R. D. (1972): Studies in intermicrobial symbiosis. *Saccharomyces cerevisiae* and *Lactobacillus casei*. – Can. J. Microbiol. **18:** 1733–1742.

Sandvik, G., Seip, K. L. & Pleym, H. (2002): An anatomy of interactions among species in a seasonal world. – Oikos **99:** 260–271.

Sarnelle, O. (1994): Inferring process from pattern: trophic level abundances and imbedded interactions. – Ecology **75:** 1835–1841.

Seip, K. L. & Reynolds, C. S. (1995): Phytoplankton functional attributes along trophical gradient and season. – Limnol. Oceanogr. **40:** 589–597.

– (1997): Defining and measuring species interactions in aquatic ecosystems. – Can. J. Fish. Aquat. Sci. **54:** 1513–1519.

Seip, K. L. & Pleym, H. (2000): Competition and predation in a seasonal world. – Verh. Internat. Verein. Limnol. **27:** 823–827.

Sommer, U., Gliwicz, Z. M., Lampert, W. & Duncan, A. (1986): The PEG-model of seasonal succession of planktonic events in fresh waters. – Arch. Hydrobiol. **106:** 433–471.

Thompson, J. N. (1999): The Evolution of Species Interactions. – Science **284:** 2116–2118.

Submitted: 28 October 2002; accepted: 28 March 2003.